Short- and Long-term Deformations of Ultra-high Strength Reinforced Concrete Columns Subjected to Severe Seismic Loading

T. Yamamoto
Daido University, Nagoya Japan

SUMMARY:
After subjected to severe seismic loads the longitudinal rigidity of reinforced concrete columns decrease remarkably. When once reinforced concrete columns yield, there is a risk of excessive short- and long-term vertical deformations of hinged columns due to the reduction of rigidity in the longitudinal direction. However, there is little information about these problems. An experimental investigation was performed to examine the effect of severe seismic loading on the short- and long-term vertical deformations of reinforced concrete columns. Experimental results showed that the longitudinal rigidity of reinforced concrete columns was considerably affected by the normal stress ratios. The total strains remarkably increased in the hinge zones of the columns. Although the longitudinal strains of column hinges increased largely, the long-term behaviours of the columns were stable due to sufficient lateral reinforcement. Thus if columns have sufficient lateral reinforcement, stable short- and long-term behaviours can be expected.

Keywords: Reinforced concrete column, Seismic loading, Vertical deformation, Lateral reinforcement, Creep

1. INTRODUCTION

To determine the propriety of safety and repair of the structure after receiving the severe earthquake is important. When once reinforced concrete columns yield, there is a risk of excessive short- and long-term deformations due to the decrease of the longitudinal rigidity. Although the locations of the yield hinges of frame buildings are intended to develop at the base of the first story columns, there is little knowledge on the long-term behaviours of such buildings after subjected to seismic loading. An experimental investigation was performed to ascertain the short- and long-term behaviours of reinforced concrete columns subjected to severe seismic loading.

Recently ultra-high strength concrete has been used for high-rise concrete buildings (Yamamoto, 1990, 1993). However, there is not necessarily sufficient information about the creep and shrinkage of such concrete (CEB-FIP 1990, ACI 209R-92 2008, AIJ 2009, fib 2010). In this study ultra-high strength concrete was included and examined.

2. EXPERIMENTAL PROGRAM

2.1. Specimens

The specimens are shown in Fig. 1 and Table 1. The specimens have a cross section of 250mm square, 1000mm length, 2.44% (l2-D13) gross reinforcing ratio, 1.20% (4-U6@40) or 0.50% (4-U4@40) 1atetal reinforcing ratio. Normal and Light-weight concrete were used. The specific concrete strengths were 120MPa, 30MPa and 40MPa for high-strength, normal-strength and light-weight concrete, respectively. High-strength reinforcing steel bars were used to obtain sufficient lateral confinement efficiently. The shear strength of the specimens was calculated and determined to exceed the shear corresponding to the flexural strength by Ohno-Arakawa equations (AIJ 2008). After seven days wet curing, all the specimens were stripped and stored in the laboratory. The temperature and humidity of the laboratory were affected by the ambient temperature and humidity change.

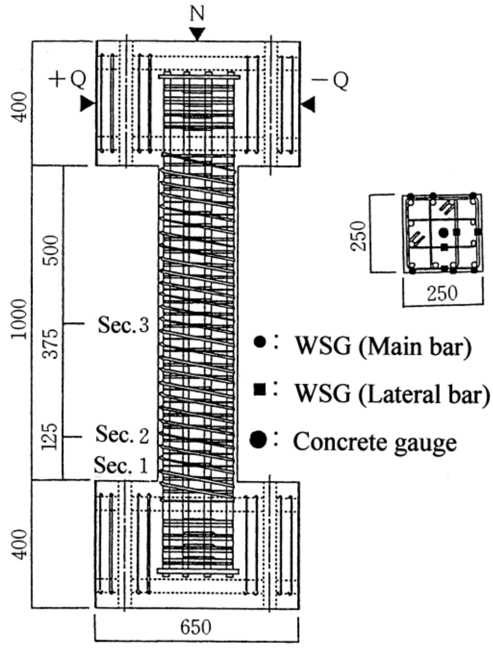

Figure 1. Specimen

Table 1. Specimens and Test Items

Specimen	Concrete (MPa)	Shape (mm)	Test Items		Normal Stress		Reinforcement	
			Seismic	Creep	Seismic	Creep	Main	Lateral
UH-1	120	250*250*1000	○	○	1/3Fc	1/3Fc	12-D13	4-U6@40
UH-2	〃	〃	−	○		1/3Fc	〃	〃
N-1	30	〃	○	○	1/3Fc	1/3Fc	〃	4-U4@40
N-2	〃	〃	○	○	2/3Fc	1/3Fc	〃	〃
L-1	40	〃	○	○	1/3Fc	1/3Fc	〃	〃
L-2	〃	〃	○	○	2/3Fc	1/3Fc	〃	〃

2.2. Materials

The mix proportions of the concrete are shown in Table 2. The mechanical properties of the concrete and reinforcing steel are shown in Table 3 and 4. The strengths of ultra-high and normal strength concrete at 28 days were 122MPa and 30.6MPa, respectively. That of light-weight concrete was 40.1MPa.

2.3 Test Procedures

2.3.1 Seismic test

In the seismic test, cyclic lateral loads were applied to the specimens at 26-28 days of the material age under a control of relative displacement angles between the top and bottom of the column specimens: single cycle at 1/1000 and 1/400, and three cycles at 1/200 and 1/l00. The relative displacement angle of 1/100 was assumed to be the limit design relative displacement angle of this test. The axial loads applied to the specimens during the seismic test were 0.33 or 0.66 of the specific concrete strength. They were 40MPa (UH-1), 10MPa (N-1), 20MPa (N-2), 13.7 (L-1) and 27.5 (L-2).

Table 2. Mix Proportion of Concrete

Concrete	Cement (kg/m^3)	Silica Fume (kg/m^3)	Water (kg/m^3)	W/(C+S) %	Aggregate (Fine, Coarse) (kg/m^3)	(kg/m^3)	Admixture
Ultra-high	610	152	160	21.0	610	910	Super Plasticizer
Normal	300	-	182	60.6	961	822	AE
Light-weight	379	-	179	47.2	771	461	AE

Table 3. Mechanical Properties of Concrete

Concrete	Age	Compressive strength (MPa)	Young's Modulus (GPa)	Specific Gravity
Ultra-high	28	122	38.6	2.43
Normal	〃	30.6	22.6	2.24
Light-weight	〃	40.1	16	1.86

Table 4. Mechanical Properties of Reinforcing Steel

Name	Diameter (mm)	Yield Point (MPa)	Tensile Strength (MPa)	Young's Modulus (GPa)	Elongation (%)	Use
D13	13	541	662	180	180	UH
D13	13	338	500	187	187	N,L
U6	6	1350	1430	221	221	UH
U4	4	1760	1940	207	207	N,L

2.3.2 Long-term creep test

The creep test was started at 28 days of material age just after the seismic test. The axial sustained load was 0.33 of the specific concrete strength, and applied to the specimens uniformly with four PC bars controlled within 3% tolerance with load-cells. The creep loads were 40MPa, 10MPa and 13.7MPa for UH, N and L series, respectively.

2.3.3 Measurement of displacement and strain

The vertical deformations of the specimens were measured with the displacement transducers. The strains of steel bars were measured at the section 1 (at the column end and embedded half of the gauge length into the stub), section 2 (12.5cm above the column end) and section 3 (centre of the column), respectively as shown in Fig. 1.

At each section strain of concrete was measured with the embedded type 10cm length gauge. The strains of longitudinal steel bars and lateral reinforcing steel bars were measured with wire-strain 4-gauges at 4 corners and wire-strain 2-gauges at 3 pints, respectively. The initials of all strains were at seven days just before stripping.

3. EXPERIMENTAL RESULTS

3.1 Seismic Test

The rigidity change and column shortening are shown in Table 5. The maximum concrete and steel strain are shown in Table 6 and Fig. 2 and Fig. 3. The column shortening ratios after seismic test (Ds/D_{cal}: elastic shortening) versus normal stress ratios are shown in Fig. 4. The load-displacement (lateral and vertical) curves of the specimen UH-1, N-1 and N-2 are shown in Fig. 5 and Fig. 6, respectively.

3.1.1 Seismic behaviour of specimen UH-1

The rigidity of the specimen decreased remarkably in the section 1 and 2 where the yield hinge was formed. The maximum compressive concrete strain of UH-1 was $3{,}070*10^{-6}$ in the section 2. The longitudinal bars yielded both in the section 1 and 2 and formed yield hinges at the top and bottom of the specimen. The maximum steel tensile strains of spirals and sub-ties were $1{,}130*10^{-6}$ and $1{,}400*10^{-6}$, respectively. They left large margin to the yield strain. The specimen UH-1 had a 0.59mm column shortening at the completion of the seismic test. Therefore the average residue strain of the specimens was $590*10^{-6}$. The shortening was about 0.6 times as much as the calculated elastic

Table 5. Rigidity Change and Column Shortening

Specimen	Maximum strength (kN)			Ec: Initial (GPa)			Ec: Unloading (GPa)			Ds: Shortening
	+Q	-Q	Q_{cal}	Sec.1	Sec.2	Sec.3	Sec.1	Sec.2	Sec.3	(mm)
UH-1	455	445	530	53.8	29.8	32.2	29.7	18.2	31.3	0.59
N-1	180	176	174	22.5	20.0	26.5	10.1	8.33	24.5	0.52
N-2	182	173	183	20.4	16.7	21.0	18.0	12.0	17.3	5.82
L-1	206	206	211	27.8	20.0	20.4	16.2	11.0	20.7	0.63
L-2	175	196	219	22.6	16.9	17.3	13.9	-	16.8	3.99

Table 6. Maximum Concrete and Steel Strain

Specimen	Concrete ($*10^{-6}$)			Steel ($*10^{-6}$)		
	Sec.1	Sec.2	Sec.3	Long.	Spiral	Sub-tie
UH-1	1,700	3,070	1,580	20,300	1,130	1,400
N-1	1,840	2,200	636	22,200	885	938
N-2	9,380	16,300	2,010	27,200	1,890	2,920
L-1	1,480	2,110	859	24,500	1,010	716
L-2	5,990	29,000	2,430	25,600	3,330	8,660

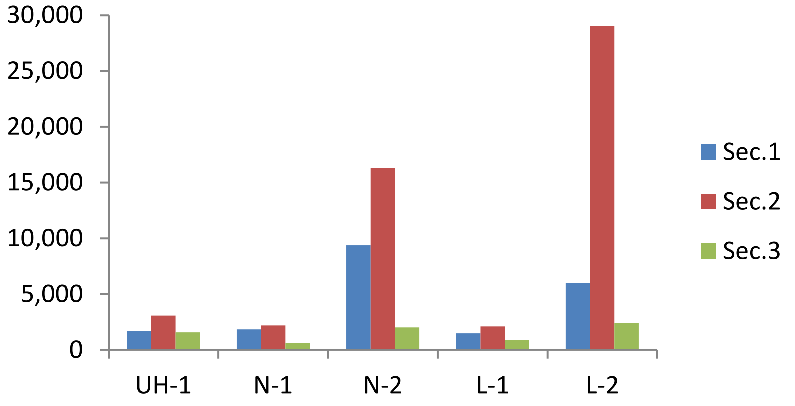

Figure 2. Maximum Concrete Strain

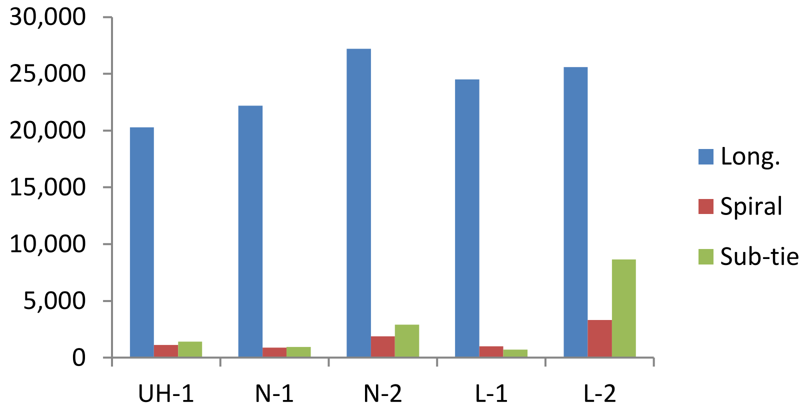

Figure 3. Maximum Reinforcing Steel Strain

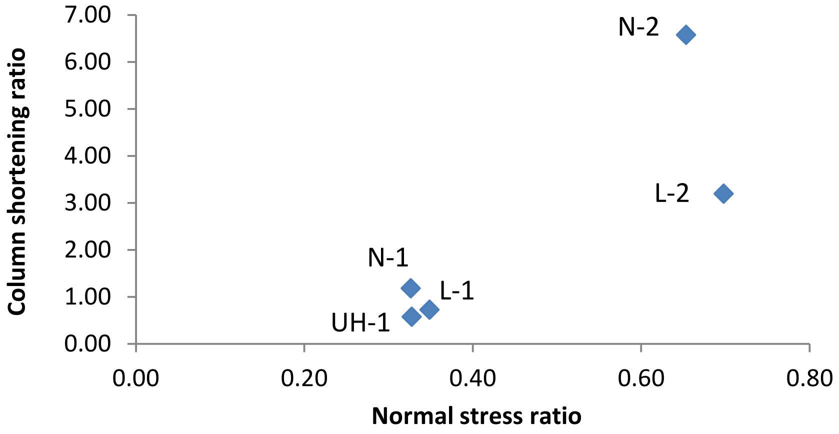

Figure 4. Column Shortening Ratios versus Normal Stress Ratios

shortening of the column subjected to 0.33 Fc normal stress.

3.1.2 Seismic behaviours of specimens N-1, N-2

The rigidity of the specimens decreased remarkably in the section 1 and 2 where the yield hinges were formed. The maximum compressive concrete strains of N-1 and N-2 were $2{,}200 \times 10^{-6}$ and 16.300×10^{-6} in the section 2, respectively. The longitudinal bars yielded both in the section 1 and 2. The maximum tensile strains of lateral reinforcing steel of N-1 and N-2 were 938×10^{-6} and $2{,}920 \times 10^{-6}$, respectively. They left also large margin to the yield strain. The specimens N-1 and N-2 had 0.52mm and 5.82mm column shortenings at the completion of the seismic test, respectively. The average residue strains of the specimens N-1 and N-2 were 520×10^{-6} and 5820×10^{-6}, respectively. They were about 1.2 and 6.6 times as much as those of the calculated elastic deformations, respectively. The axial load ratios affected both the maximum steel strains and column shortenings largely.

3.1.3 Seismic behaviours of specimens L-1, L-2

The rigidity of the specimens decreased remarkably in the section 1 and 2 where the yield hinges were

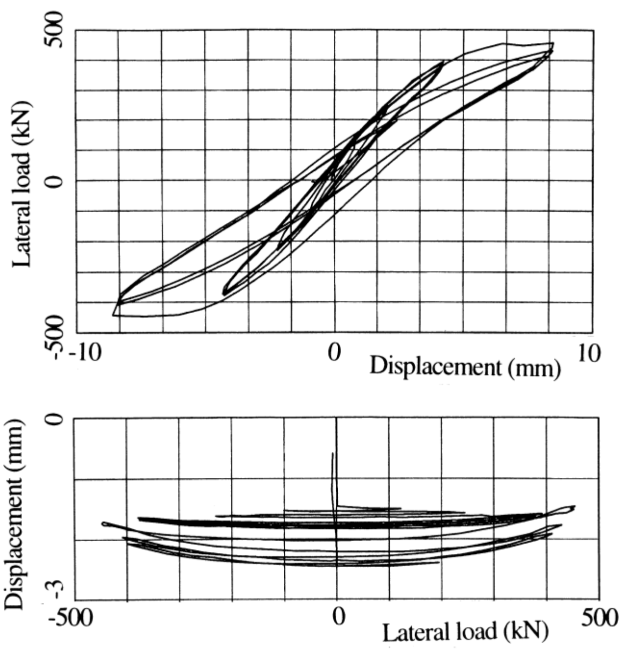

Figure 5. Load-displacement (lateral and vertical) Curves of Specimen UH-1

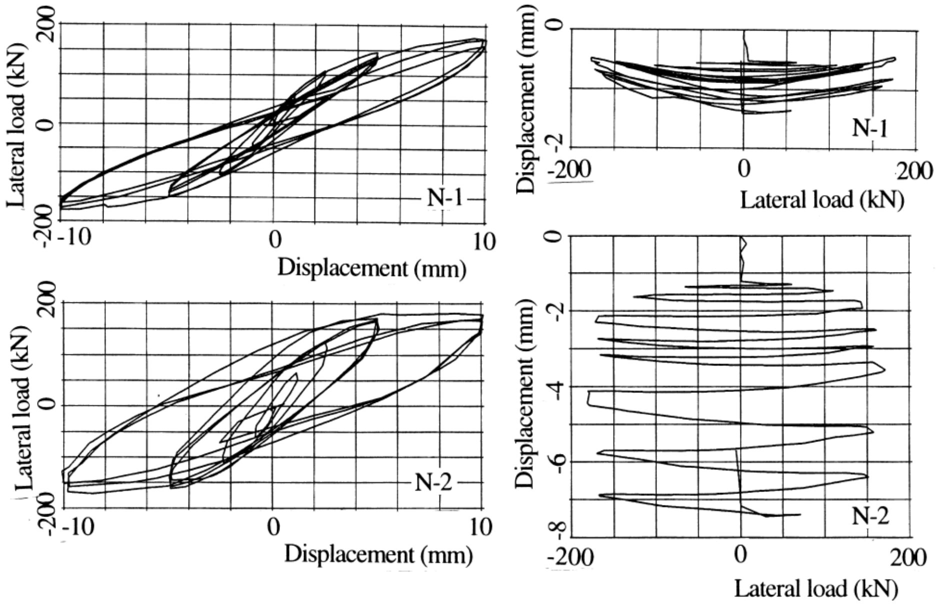

Figure 6. Load-displacement (lateral and vertical) Curves of Specimen L-1 and L-2

formed. The maximum compressive concrete strains of L-1 and L-2 were $2,110*10^{-6}$ and $29,000*10^{-6}$ in the section 2, respectively. The longitudinal bars yielded both in the section 1 and 2. The maximum tensile strains of lateral reinforcing steel of L-1 and L-2 were $1,010*10^{-6}$ and $3,330*10^{-6}$, respectively. The specimens L-1 and L-2 had 0.72mm and 3.19mm column shortenings at the completion of the seismic test, respectively. The average residue strains of the specimens L-1 and L-2 were $720*10^{-6}$ and $3190*10^{-6}$, respectively. They were about 0.7 and 3.2 times as much as those of the calculated elastic deformations, respectively. The axial load ratios affected both the maximum steel strains and column shortenings largely.

3.2 Creep Test

Results of the creep test are shown in Table 7. Total strain ratios of the specimens are shown in Table 8. Changes in strains of the specimens at each section of specimens UH, and N series are shown in Fig. 7 and Fig. 8, respectively.

Table 7. Results of Creep Test

Specimen	Ec: Loading (GPa)			Strain at loading ($*10^{-6}$)			Strain increment ($*10^{-6}$)			Increment factor		
	Sec.1	Sec.2	Sec.3	Sec.1	Sec.2	Sec.3	Sec.1	Sec.2	Sec.3	Sec.1	Sec.2	Sec.3
UH-1	35.4	20.7	33.2	1,130	1,930	1,210	1,050	1,420	1,080	0.93	0.74	0.89
UH-2	45.8	33.4	37.2	874	1,200	1,080	1,020	1,190	1,170	1.17	0.99	1.08
N-1	10.6	8.00	21.2	935	1,220	462	607	819	674	0.66	0.67	1.46
N-2	16.9	11.4	15.1	579	860	618	787	1,100	741	1.36	1.28	1.14
N-1	18.1	11.8	20.1	763	1,164	682	537	756	666	0.70	0.65	0.98
N-2	17.6	-	16.1	781	250	854	425	401	689	0.54	1.60	0.81

Table 8. Total Strain

Specimen	Strain at 28 days (μ)			Total strain (μ)			Total strain ratio (/Sec3)		
	Sec.1	Sec.2	Sec.3	Sec.1	Sec.2	Sec.3	Sec.1	Sec.2	Sec.3
UH-1	537	1,390	574	2,710	4,740	2,970	0.91	1.60	1.00
UH-2	166	205	193	2,060	2,590	2,440	0.84	1.06	1.00
N-1	224	927	774	1,360	2,960	2,300	0.59	1.29	1.00
N-2	809	14,000	7,740	2,200	16,000	9,100	0.24	1.76	1.00

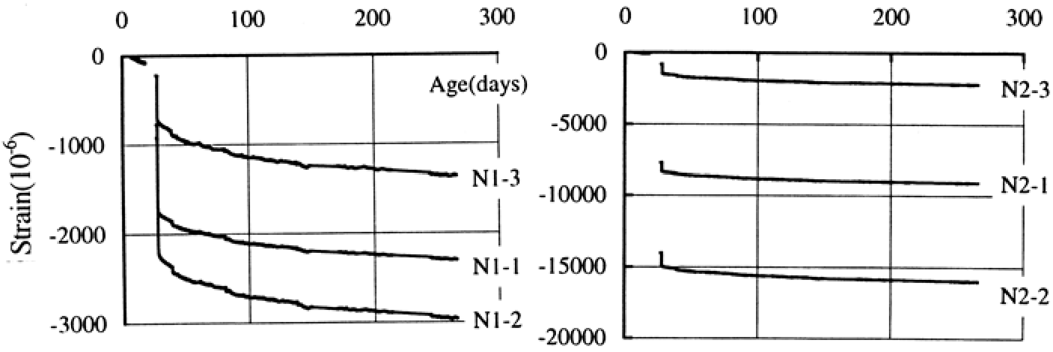

Figure 7. Change in Concrete Strain of UH-1 and UH-2

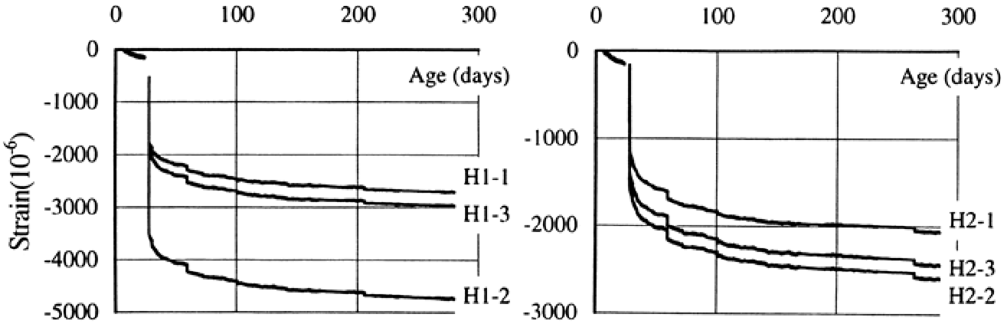

Figure 8. Change in Concrete Strain of N-1 and N-2

3.2.1 Change in Vertical rigidities and Strains of Specimens UH-1, UH-2

The rigidities of the specimen UH-1 and UH-2 in the section 2 at the completion of the creep loading were 20.7GPa and 33.4GPa, respectively. The axial rigidity of the specimen UH-1 was remarkably reduced compared with that of the specimen UH-2. The total concrete strains of UH-1 and UH-2 in the section 2 at the age of 286 days reached up to $4{,}740*10^{-6}$ and $2{,}590*10^{-6}$, respectively. The total strains of UH-2 were about 2.4 times as much as that of the calculated elastic strain. Therefore the increment strain factor of UH-2 was 1.4 and much smaller than that of normal strength concrete. Although the total strain of the specimen UH-1 in the section 2 was much larger than that of UH-2, the long-term behaviours were stable.

3.2.2 Change in Vertical rigidities and Strains of Specimens N-1, N-2

The rigidity of the specimen N-1 and N-2 in the section 2 at the completion of the creep loading were 8.04GPa and 11.4GPa, respectively. The axial rigidities were remarkably reduced. The total concrete strains of N-1 and N-2 in the hinged section at the age of 266 days reached up to $2{,}960*10^{-6}$ and $16{,}000*10^{-6}$, respectively. They were much larger than that of the non-hinged section 3. The maximum strain of N-2 was about the same as that measured at the seismic test. The long-term behaviours of N-2 showed stable. It was found that the axial load ratio during the seismic test greatly affected the longitudinal rigidity of the columns. Although the strain at the hinged section of N-2 became considerably large, the long-term behaviours were stable due to sufficient lateral reinforcement.

3.2.3 Change in Vertical rigidities and Strains of Specimens L-1, L-2

The rigidity of the specimen L-1 in the section 2 at the completion of the creep loading was 11.8GPa. The axial rigidities were remarkably reduced. The total concrete strains of L-1 and L-2 in the hinged section at the age of 274 days reached up to $2{,}650*10^{-6}$ and $29{,}200*10^{-6}$, respectively. They were much larger than that of the non-hinged section 3. The long-term behaviours of L-1 and L-2 showed stable. It was found that the axial load ratio during the seismic test greatly affected the longitudinal rigidity of the columns. Although the strain at the hinged section of L-2 became considerably large, the long-term behaviours were stable due to sufficient lateral reinforcement

3.2.4 Creep strain increment ratio and total strain

Fig. 9 shows the creep strain increment ratio versus normal stress ratio at the seismic test. Fig. 10 shows the total strain of Sec. 2. The creep strain increment ratios of high normal stress ratio specimens at the seismic test indicate greater value than those of the low normal stress ratio. Although the total strain of high normal stress ratio specimens at the seismic test increased up to $30{,}000{*}10^{-6}$, the long-term behaviours were stable without significant increase of creep strain.

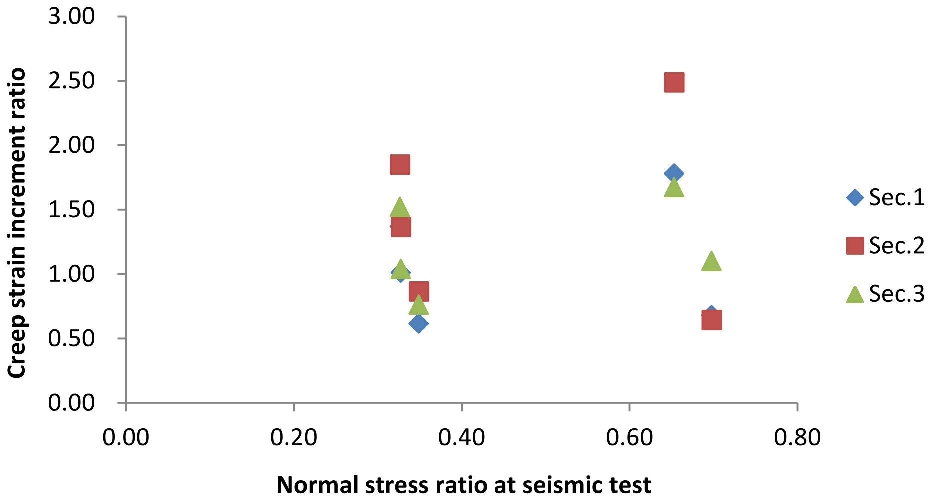

Figure 9. Creep Strain Increment Ratio versus Normal Stress Ratio at Seismic Test

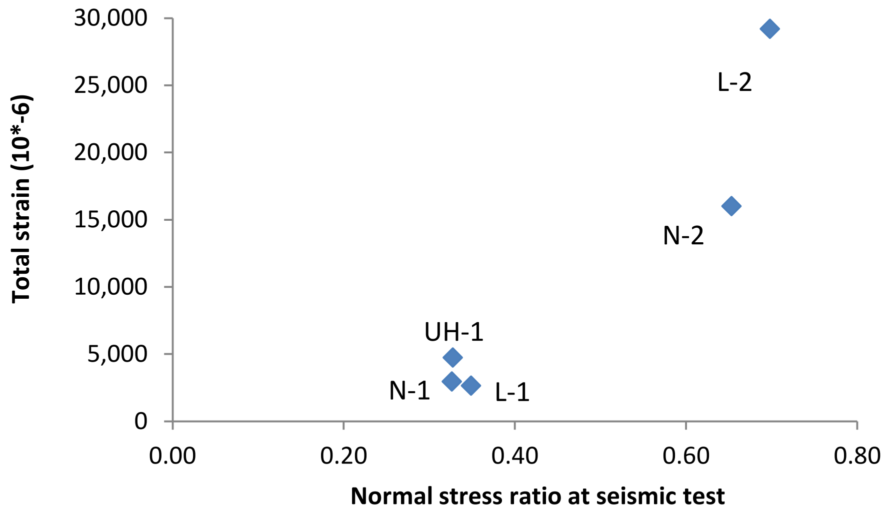

Figure 10. Total Strain of Sec. 2 versus Normal Stress Ratio at Seismic Test

4. CONCLUSIONS

The following conclusions are derived from the tests results described in this paper.

1) The shortenings of UH-1, N-1 and L-1 column specimens subjected to seismic loading with the 1/l00 relative displacement angle under 0.33Fc (40MPa and 10MPa) axial load were 0.59mm, 0.52mm, and 0.63mm respectively. They were about 0.6, 1.2 and 0.7 times as much as those of the calculated elastic deformations, respectively.
2) The shortening of N-2 and L-2 column specimen subjected to the same seismic loading under 0.66fc (20MPaand 28MPa) axial load were 5.82mm and 3.99mm, respectively. They were 6.6 and 3.19 times as much as that of the calculated elastic deformation, respectively. They were much

larger than those of UH-1 and N-1.

3) The strain increment factor of the ultra-high strength concrete column specimen UH-2 was about 1.4 and much smaller than that of normal strength concrete.
4) The total strains remarkably increased in the hinge zones of the columns. The seismic loading was responsible for the decrease in the axial rigidities and increase in the residual strains.
5) Although the total creep strain of high normal stress ratio specimens at seismic test increased up to $30{,}000*10^{-6}$, the long-term behaviours were stable without significant increase of creep strain.
6) Due to high strength sufficient lateral reinforcement, the long-term behaviors of the columns subjected to the seismic loading were stable. Thus if columns have sufficient lateral reinforcement stable short and also long-term behaviors can be expected.

AKCNOWLEDGEMENT

The author thanks to Mr. T. Iwakura and Dr. T. Ohtaki who cooperated in the study.

REFERENCES

ACI 209R-92 (2008), Prediction of Creep, Shrinkage, and Temperature Effects in Concrete Structures.

AlJ (2009), State-of-the-Art Report on High Strength Concrete, Architectural Institute of Japan, Maruzen, Tokyo

AlJ (2008), Standard for Structural Calculation of Reinforced Concrete Structures, Architectural Institute of Japan, Maruzen, Tokyo

CEB-FIP (1990), Model Code1990, Thomas Telford, London

Fib (2010), Model Code2010, Federation International du Beton, Lausanne

Yamamoto, T. (1990), Creep and Shrinkage of High-Strength Reinforced Concrete Columns, *Transactions of Japan Concrete Institute*, 12, 101-106.

Yamamoto, T. (1993), Creep and Shrinkage of 150MPa Ultra-High Strength Reinforced Concrete Columns, *Transactions of Japan Concrete Institute*, 15, 109-114.